Available online at www.sciencedirect.com
SCIENCE DIRECT®
Precambrian Research 127 (2003) 103–123
Precambrian Research
www.elsevier.com/locate/precamres

Late Archaean granites: a typology based on the Dharwar Craton (India)

J.-F. Moyen [a,*], H. Martin [a], M. Jayananda [b], B. Auvray [c,✠]

[a] *Laboratoire Magmas et Volcans, OPGC—Université Blaise Pascal—CNRS, 5, rue Kessler, 63038 Clermont-Ferrand Cedex, France*
[b] *Department of Geology, Bangalore University, Bangalore, Karnataka, India*
[c] *Géosciences Rennes, Université Rennes-1, and CNRS Rennes, France*

Accepted 10 April 2003

Abstract

Extensive field work in the Eastern Dharwar Craton, associated with petrographic and geochemical (major and trace elements) investigations, allows four main types of Late Archaean granitoids to be distinguished. (1) Na-rich granitoids of trondhjemitic, tonalitic and granodioritic composition (TTG) that are characterised by strongly fractionated REE patterns and low HREE contents and generally interpreted as "slab melts" generated by partial melting of metamorphosed hydrated basalt, most likely in a subduction environment. (2) Sanukitoids, which are K- and Mg-rich monzonites and granodiorites with TTG-like REE patterns associated with marked LILE-enrichment, and considered to result from the reaction of slab melts generated in a subduction environment with, and assimilation of, mantle wedge peridotite. (3) Uncommon high-HFSE, Mg and K granites with strongly REE and LILE-enrichment that, probably formed by partial melting of an enriched mantle source; unlike in the genesis of sanukitoids, in this case the slab melt is considered to be wholly consumed by reaction with mantle minerals, resulting in mantle-enrichment. Subsequent melting of this enriched mantle (probably in a post-subduction setting) gives rise to high-HFSE, Mg and K magmas. As demonstrated for the Closepet Granite (Dharwar Craton), the hot mantle-derived magma can induce melting of continental crust and then mix with the anatectic products. (4) K-rich, Mg-poor anatectic biotite-granites with REE patterns that are less fractionated and show negative Eu anomalies. These granites result from the remelting of old basement or recently accreted plutons, both with TTG compositions. Such anatexis can occur either in a subduction or in a post-subduction environment.

This typology, based on the well-exposed Dharwar Craton, can be extended to Late Archaean granitoids from all over the world. About such 500 analysis were compiled, and a number of discriminant diagrams, based on both major and trace elements, are proposed. The most likely tectonic setting for the observed rock types is an accretionary orogen with accretion of continental blocks above a subduction system, followed by thermal reworking of the newly accreted continental material. However, it has been found that Archaean "subduction-related" granitoids are significantly different from their modern counterparts, implying progressive changes in the modes of magma generation at convergent margins from the Archaean to the present.

Keywords: Dharwar Craton; Late Archaean granites; Granite typology; Sanukitoids; TTG

* Corresponding author. Present address: UMR 5570, Université Claude Bernard—Lyon I, 2 Rue Raphaël Dubois, 69622 Villeurbanne Cedex, France. Tel.: +33-4-72-446242; fax: +33-4-72-448593.
E-mail address: jfmoyen@wanadoo.fr (J.-F. Moyen).
✠ Deceased.

0301-9268/$ – see front matter © 2003 Elsevier B.V. All rights reserved.
doi:10.1016/S0301-9268(03)00183-9

1. Introduction

Archaean cratons are commonly composed of three main lithologic units (Windley, 1995): (1) a gneissic basement of tonalitic–trondhjemitic–granodioritic (TTG) composition; (2) volcano-sedimentary basins, known as "greenstone belts"; (3) K-rich granites, generated generally late in the geological evolution of the craton. Among these three classical lithologies, two (TTG and greenstone belts) have been extensively studied in the past decades. However, the late, K-rich granites have drawn relatively less attention. Until ten years ago, it was commonly assumed that all late granites were related to intra-crustal anatexis; compositional differences were attributed to the depth of melting, or to the nature of the source (e.g. Sylvester, 1994). However, this view was challenged by Shirey and Hanson (1984), who reported and studied a group of rocks, referred as "sanukitoids", which display evidence of a (at least partially) mantle-derived origin. Furthermore, increasing evidence of the involvement of old continental crust and/or mantle in the genesis of some TTG (e.g. Berger and Rollinson, 1997) further complicated this simplistic understanding, demanding a re-examination of the models for the formation of Archaean plutonic rocks.

A review of published data suggests there are five main types of Archaean granitoids:

(1) TTG is the most common Archaean plutonic suite. It constitutes the gneissic basement of all cratons (Windley, 1995), representing up to 60–80% of their overall volume. Occasionally, TTG rocks also form individual, well-defined syn- to post-tectonic plutons (Champion and Smithies, 1999; Day and Weiblen, 1986; Shirey and Hanson, 1986; Stevenson et al., 1999). The TTG suite is characterised by sodium-enrichment ($K/Na < 0.3$) and strongly fractionated REE patterns ($[Ce/Yb]_N = 10–40$) with no significant Eu anomaly (see Martin, 1994 for review). Today, most researchers agree that TTG magmas were generated by partial melting of hydrous basalt leaving a garnet-bearing or an eclogitic residue. These conclusions are supported by geochemical modelling (Martin, 1986, 1994; Martin and Moyen, 2002) and experimental petrology (Rapp, 1994; Sen and Dunn, 1994; Zamora, 2000), as well as by the study of modern analogues such as adakites (Defant and Drummond, 1990; Martin, 1999). In contrast, the geodynamic setting where TTG magmas were generated and emplaced is still subject to controversy and debate (e.g. De Wit, 2001). Some believe that TTG are produced by partial melting of subducted, basaltic oceanic crust (Condie, 1989; Martin, 1986, 1994; Rollinson, 1997; Albarède, 1998; Martin and Moyen, 2002). Others contend that TTG are generated by melting of basalt at the base of a thickened continental crust, and that the basalt was either underplated through magmatic processes (Atherton and Petford, 1993; Rudnick, 1995; Albarède, 1998) or underthrust during flat subduction (Smithies, 2000).

(2) Biotite-bearing granites probably represent the second most abundant family. Most of the "Late Archaean, K-rich plutons" belong to this type (see Sylvester, 1994 for review). They are biotite- (and rarely hornblende-) bearing monzo- to syenogranites to granodiorites, with high K/Na ratios (>1), moderately fractionated REE patterns ($[Ce/Yb]_N < 30$) and a significant negative Eu anomaly. In many places, these granites have been demonstrated to be products of partial melting of pre-existing TTG gneisses (Querré, 1985; Jahn et al., 1988; Collins, 1993; Champion and Sheraton, 1997; Frost et al., 1998; Champion and Smithies, 1999).

(3) The term "sanukitoids" was proposed by Shirey and Hanson (1984) to describe a family of rocks initially identified in the Late Archaean Superior Province of Canada. These authors defined sanukitoids as diorites to granodiorites with high Mg# (>70), associated with high Ni and Cr contents; they are also alkali and LILE-rich ($Na_2O + K_2O > 3\%$ for $SiO_2 = 50\%$; $Ba > 800$ ppm; $Sr > 800$ ppm). REE patterns are strongly fractionated ($[Ce/Yb]_N = 10–50$) with high LREE contents ($Ce_N > 100$) and no, or slightly negative, Eu anomalies. Sanukitoids are rather common in the Superior Province (Shirey and Hanson, 1984, 1986; Stevenson et al., 1999; Stern and Hanson, 1991) and more recently have been described in South India (Balakrishnan and Rajamani, 1987; Krogstad et al., 1995), in the Pilbara Craton (Smithies and Champion, 1999)

and in China (Jahn et al., 1988). The question of their origin is still widely debated. While most workers agree that both mantle and an arc-related component must play a role in their formation, two main hypotheses have been proposed for their petrogenesis: (a) melting of enriched mantle, whose source of enrichment is assumed to be either subduction-released fluids (as in modern calc-alkali magmas: Balakrishnan and Rajamani, 1987; Stern et al., 1989; Stern and Hanson, 1991; Krogstad et al., 1995), or the so-called "slab melts", which are partial melts of hydrous basalt in the garnet stability field (i.e. TTG magmas; Smithies and Champion, 1999); (b) assimilation of mantle peridotite by slab melts ascending through the mantle wedge (Rapp et al., 2000).

(4) Archaean leucogranites, peraluminous granites and "S-type" granites are occasionally reported. They are muscovite-bearing (and rarely garnet-bearing) leucogranites with high K/Na ratios (up to 2.5), moderately fractionated REE patterns ($[Ce/Yb]_N < 30$), with a strong negative Eu anomaly, and Rb- and Th-rich. Invariably, this type of granite has been demonstrated to be a product of partial melting of metasediments (Day and Weiblen, 1986; Frost et al., 1998).

(5) Minor occurrences of peralkaline granites and syenites have also been reported from the Superior Province (Laflèche et al., 1991; Bourne and L'Heureux, 1991), Yilgarn Craton (Champion and Sheraton, 1997) and Pilbara Craton (Champion and Smithies, 1999).

The Eastern Dharwar Craton (EDC), in South India, was accreted during the Late Archaean (2.7–2.5 Ga; see Chadwick et al., 2000 for review). The EDC contains large amounts of late potassic granites belonging to most of the different types described above, and are chronologically and spatially associated with the emplacement of large volumes of TTG magmas (Jayananda et al., 2000). This area thus provides a good opportunity to study the various types of Late Archaean granites, their relationships, and their possible petrogenetic links in a single crustal segment. The conclusions drawn from this study of the EDC will then be tentatively extended to the whole Late Archaean.

2. Geological setting

The Dharwar Craton of South India consists of two parts; (1) the older Western Dharwar Craton (WDC; 3.3–2.7 Ga), and (2) the younger EDC (3.0–2.5 Ga) (Chadwick et al., 2000, and references therein). The WDC mainly comprises a TTG gneissic basement overlain by greenstone belts, whereas the EDC is made up of Late Archaean (2.6–2.5 Ga) granites intrusive into subordinate amounts of older (2.9–2.7 Ga) TTG gneisses. Greenstones in the EDC are confined to small, elongated belts which may represent terrane boundaries (Krogstad et al., 1989; Chadwick et al., 2000).

The Dharwar Craton represents a cross-section through the Archaean crust, which has been tilted after 2.5 Ga (Rollinson et al., 1981; Raase et al., 1986; Chadwick et al., 2000). Hence, deep structural levels (up to granulite facies) crop out in the southern part of the craton, and shallower levels are found towards the north. Within the studied area (see Fig. 1), rocks of the Dharwar Craton are at amphibolite facies and overlain on the northern margin by Proterozoic sediments of the Cuddapah Basin. Late Archaean granitoids are found in two settings in the EDC (Fig. 1). In the deeper, southern part of the craton at granulite to upper amphibolite facies, granites occur as an intricate pattern of sheets, dykes and plugs of diverse composition and are interpreted as due to underplating and injections at the base of a continental fragment (Allen et al., 1985; Peucat et al., 1993). On the other hand, at shallower levels further north, granites form discrete, mappable plutons. Most of these are elongated, consistent with emplacement along active shear zones, as demonstrated in the case of the Closepet Granite (Moyen et al., 2003). The largest of these intrusions extends over 400 km from south to north.

3. Granite types

Four main Late Archaean granitoid types have been identified in the Dharwar Craton, based on petrography (Fig. 2, Table 1) and major and trace element geochemistry (Tables 2 and 3 and Figs. 3–7). Three granite types (TTG, sanukitoids and biotite-granites) correspond to types already described elsewhere in the literature, whereas the fourth one (Closepet Granite)

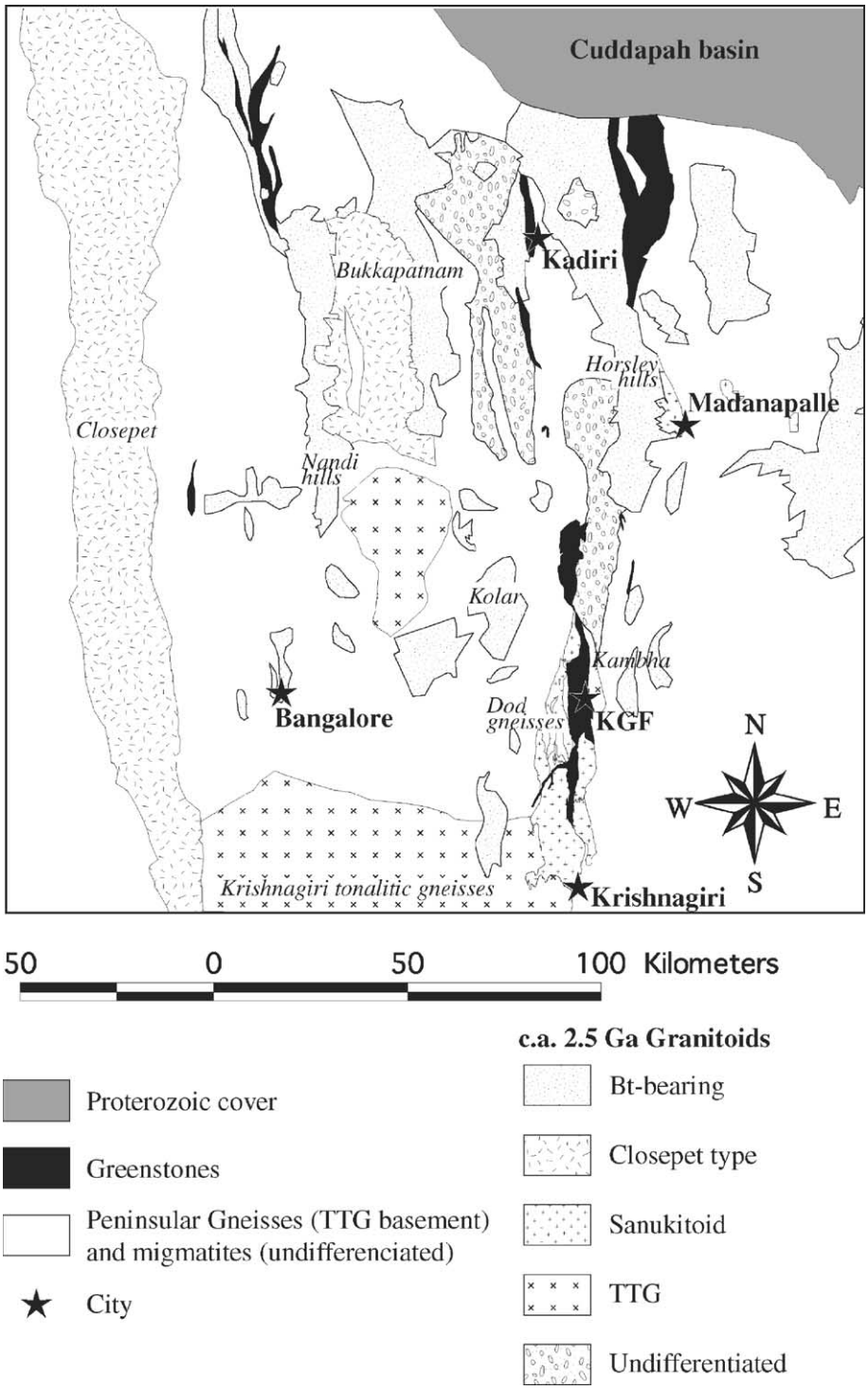

Fig. 1. Geological sketch map of the EDC, showing the distribution of the studied types of granitoids.

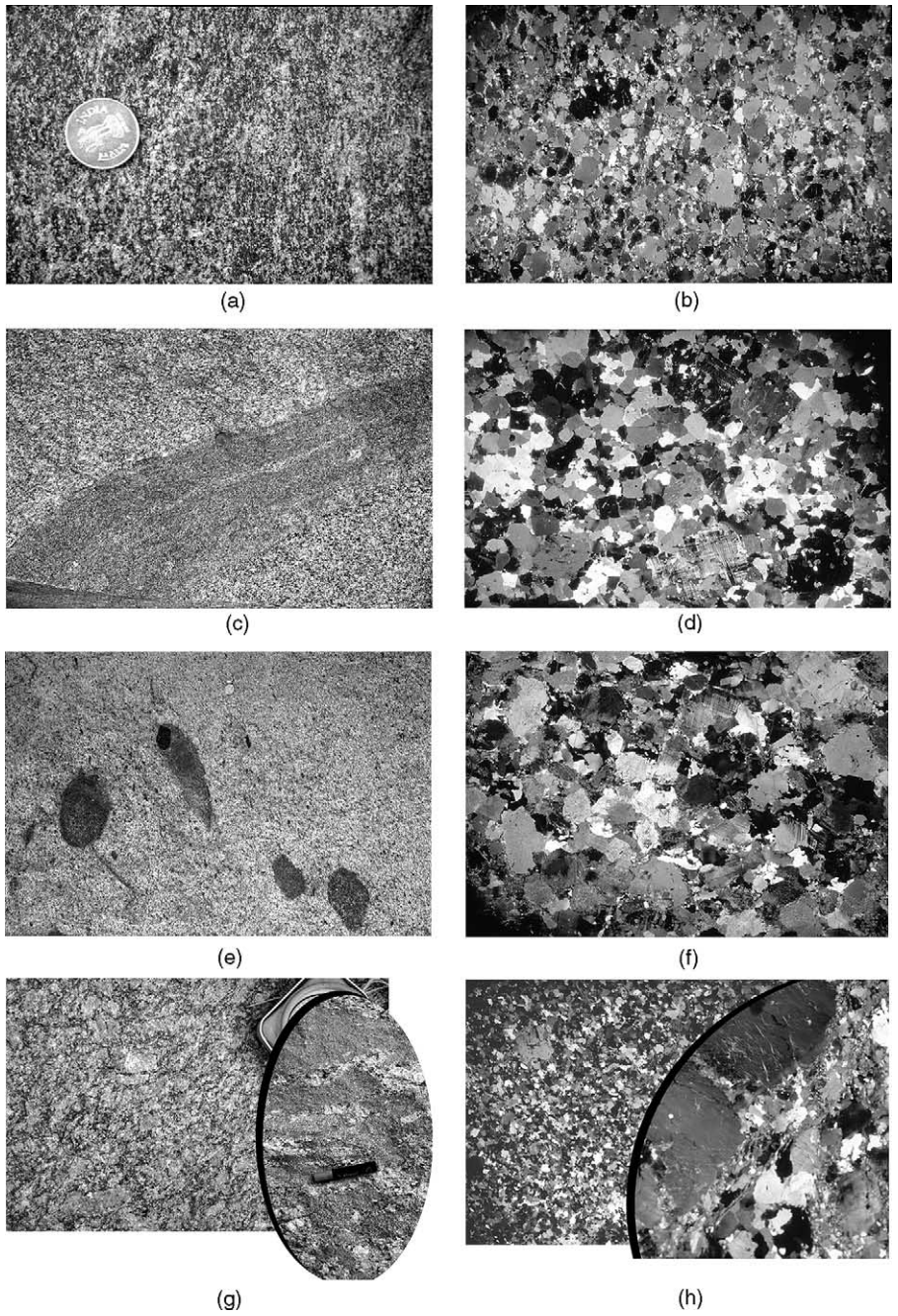

Fig. 2. Field and thin section (crossed polar) photographs of the four types of granitoids in the EDC. (a) Krishnagiri tonalitic gneisses. (b) Photomicrograph of (a). (c) Two comagmatic facies of biotite-bearing granites, Southern part of Lepakshi granite. (d) Photomicrograph of (c). (e) "Dod gneiss" sanukitoid, East of Kolar Schist Belt. (f) Photomicrograph of (e). (g) Dominant, porphyritic facies of the Closepet Granite, with mingling features with the diorite in inset. (h) Photomicrograph of Closepet dioritic phase (inset: porphyritic phase). Scale bar of field photographs ≈20 cm. Width of photomicrographs ≈2 cm.

Table 1
Petrological, mineralogical and major element characteristics for the six Late Archaean granite types discussed in this paper

Type	Rock types	Fe–Mg minerals	Accessory minerals	Other common characteristic	Mg#	A/CNK	K/Na
TTG	Trondhjemite, tonalite, granodiorite	Bt, Hb	Mt, Ilm, Ap, Sph, Zn, All, Ep		35–50	0.9–1.3	**<0.4**
Sanukitoids	Monzodiorite, granodiorite	Bt, Hb (Cpx)	Mt, Ilm, Ap, Sph, Zn, All	Mafic clusters of Hb + Bt ± Cpx; MME	**45–75**	0.8–1.2	0.4–0.7
Closepet-like	Diorite, granodiorite (granite)	Bt, Hb (Cpx)	Mt, Ilm, Ap, Sph, Zn, All	Commonly porphyritic; associated with anatectic granites; lot of MME	35–70	0.3–0.9	0.45–0.9
Biotite-granites	Granodiorite, granite	Bt (Hb)	Mt, Ilm, Ap, Zn	Restitic enclaves, pegmatites; Sometimes associated with migmatites	20–40	**1.0–1.4**	1.0–2.5
Two-mica granites	Granite (leucogranite)	**Bt, Ms (Gt)**	Ilm, Zn	Restitic enclaves; Sometimes associated with migmatites	20–40	**1.3–1.6**	1.0–2.5
Peralkaline	Granite	**Bt, Na–Px**	?		20–35	0.8–1.0	0.3–0.6

Note that only four of them (TTG, sanukitoids, Closepet-type and biotite-granites) are present in the Dharwar Craton. Mineral names: Bt, biotite; Hb, hornblende; Cpx, Clinopyroxene; Ms, Muscovite; Gt, Garnet; Na–Px, Sodic pyroxene (e.g. Riebeckite); Mt, Magnetite; Ilm, Ilmenite; Ap, Apatite; Sph, Sphene; Zn, Zircon; All, Allanite; Ep, other epidote. MME, microgranular mafic enclave. Chemical ratios: Mg# molecular ratio$100 \times Mg/(Mg + Fe)$; A/CNK molecular ratio $Al/(Ca + Na + K)$; K/Na molecular ratio. Most discriminant features are in bold.

Table 2
Trace elements for the 6 Late Archaean granite types discussed in the paper

Type	REE	HFSE	Rb & Th	LILE	Transition elements
TTG	**Ce_N = 50–150, Yb_N = 1–5, $[Ce/Yb]_N$ = 10–40, Eu/Eu*: no**	Nb = 1–10, Zr = 100–150, Y = 1–10	Rb = 5–50, Th = 1–5	Sr = 200–800, Ba = 100–1000	Ni = 5–30, Cr = 5–50
Sanukitoids	Ce_N = 100–200, Yb_N = 1–10, $[Ce/Yb]_N$ = 10–50, Eu/Eu*: slightly negative	Nb = 5–10, Zr = 100–200, Y = 5–20	Rb = 50–150, Th = 5–20	Sr = 400–1000, Ba = 500–2000	Ni = 20–60, Cr = 20–150
Closepet-like	Ce_N = 150–400, Yb_N = 5–20, $[Ce/Yb]_N$ = 10–50, Eu/Eu*: slightly negative	**Nb = 10–20, Zr = 200–400, Y = 20–40**	Rb = 50–150, Th = 5–20	Sr = 500–1500, Ba = 800–2000	Ni = 10–30, Cr = 20–50
Biotite-granites	Ce_N = 50–200, Yb_N = 5–10, $[Ce/Yb]_N$ = 10–30 Eu/Eu*: negative	Nb = 1–20, Zr = 100–200, Y = 1–20	**Rb = 150–250, Th = 10–60**	Sr = 150–600, Ba = 400–1200	Ni = 1–10, Cr = 5–20
Two-mica granites	Ce_N = 20–80, Yb_N = 2–10, $[Ce/Yb]_N$ = 10–30, Eu/Eu*: strongly negative	Nb = ?, Zr = 50–150, Y = ?	**Rb = 100–150, Th = 5–20**	Sr = 100–200, Ba = 600–1200	Ni =?, Cr = ?
Peralkaline	Ce_N = 100–250, Yb_N = 3–5, $[Ce/Yb]_N$ = 25–50, Eu/Eu*: slightly negative	Nb = 1–10, Zr = 50–200, Y = 10–30	Rb = 50–200, Th = 10–20	Sr = 800–1200, Ba = 800–2000	Ni = 1–5, Cr = 5–10

Eu/Eu^* calculated as $Eu/((Sm + Gd) \times 0.5)$. REE: chondrite-normalized values; other elements; PPM.

Table 3
Selected chemical analyses for granites of the four types of the Dharwar Craton, with references

Sample # nature	TTG		Bt-bearing granites		Sanukitoids		Closepet-type					
	24[a]	27[a]	BH23[b]	BH25a[b]	87/S7[c]	87/S20[c]	J1[d]	J9[d]	CG9[d]	CG5[e]	J3[e]	J10[e]
Major elements (wt.% oxides)												
SiO_2	67.13	67.92	69.69	71.72	59.38	64.92	57.74	58.29	49.38	61.12	62.5	64.11
Al_2O_3	16.49	16.27	15.75	13.54	16.32	14.9	16.53	15.41	13.59	16.27	16.43	16.16
FeO tot	3.43	3.15	2.03	2.32	6.17	4.67	6.37	6.46	11.29	4.74	4.45	4.01
MnO	0.03	0.03	0.04	0.04	0.09	0.08	0.09	0.10	0.14	0.1	0.07	0.05
MgO	1.42	1.23	0.38	0.33	3.04	2.11	2.83	2.22	3.98	1.89	1.55	1.38
CaO	3.91	3.43	2.69	1.46	5.59	3.78	4.83	4.83	7.56	3.87	3.40	2.90
Na_2O	4.84	5.06	4.73	3.18	4.39	3.84	4.21	4.03	3.02	4.1	4.36	4.25
K_2O	1.55	1.54	2.66	5.47	1.53	2.96	3.21	4.21	1.77	4.09	4.00	4.58
TiO_2	0.47	0.47	0.26	0.43	0.7	0.44	0.97	1.13	2.82	0.79	0.69	0.61
P_2O_5	0.16	0.14	0.08	0.13	0.29	0.18	0.80	0.72	1.97	0.46	0.41	0.41
Sum	99.43	99.24	98.31	98.62	97.50	97.88	97.58	97.40	95.52	97.43	97.86	98.46
Mg#	42	41	25	20	47	45	44	38	39	42	38	38
K/Na	0.21	0.20	0.37	1.13	0.23	0.51	0.50	0.69	0.39	0.66	0.60	0.71
A/CNK	0.98	1.00	1.01	0.98	0.86	0.91	0.86	0.77	0.66	0.89	0.93	0.94
Trace elements (ppm)												
Nb	4.7	4.7	4	26	6	6	ND	ND	35	17	ND	ND
Zr	103	295	139	324	211	221	238	372	510	294	302	284
Y	5	2.8	3	37	18	18	39	37	69	44	23	24
Sr	648	595	556	270	866	866	935	1040	840	882	906	807
Rb	40	59	72	217	57	80	117	84	50	98	120	127
Ni	24	27	1	6	45	36	19	19	36	15	7	10
Cr	16	5	14	14	130	113	17	27	31	18	9	15
Ba	570	396	1312	803	682	974	985	1617	812	1202	1333	1362
Th	0.9	5	8	47	ND	ND	14	9	6	7	15	12
REE (normalized to chondrites, Sun and McDonough, 1989)												
La	73.02	120.63	131.05	426.98	160.48	119.21	326.98	349.21	ND	ND	307.94	260.32
Ce	57.81	75.03	87.50	307.13	131.37	101.48	275.52	319.80	ND	ND	226.32	200.49
Nd	ND	ND	36.55	152.40	83.37	67.34	157.45	185.93	ND	ND	108.88	98.83
Sm	14.06	13.02	15.94	73.80	38.13	33.18	77.45	88.91	ND	ND	48.85	47.45
Eu	18.01	13.85	12.33	21.47	24.93	16.62	40.05	52.21	ND	ND	28.04	25.00
Gd	ND	ND	9.38	39.38	ND	ND	36.06	38.92	ND	ND	22.90	22.36
Dy	ND	ND	4.13	20.46	ND	ND	20.40	22.22	ND	ND	12.92	12.68
Er	ND	ND	2.71	15.87	ND	ND	16.34	15.82	ND	ND	9.39	8.59
Yb	2.36	1.88	2.50	13.89	5.29	5.77	15.72	14.62	ND	ND	7.26	6.44
Lu	2.48	1.55	2.51	12.07	5.57	4.95	15.48	13.31	ND	ND	7.12	5.57
Eu/Eu*	0.76	0.71	0.97	0.38	1.31	1.00	0.71	0.82			0.78	0.72
Ce/Yb	24.5	40.0	35.1	22.1	24.8	17.6	17.5	21.9			31.2	31.1

Same abbreviations as Table 1. FeO tot, total iron calculated as FeO. Eu/Eu* calculated as $Eu/((Sm + Gd) \times 0.5)$.

[a] Krishnagiri tonalitic gneisses; Allen, 1985.
[b] Kolar intrusion; Jayananda et al., 2000.
[c] "Dod gneisses"; Reddy, 1987.
[d] Clinopyroxene-bearing monzonite; Jayananda et al., 1995.
[e] Porphyritic monzogranite; Jayananda et al., 1995.

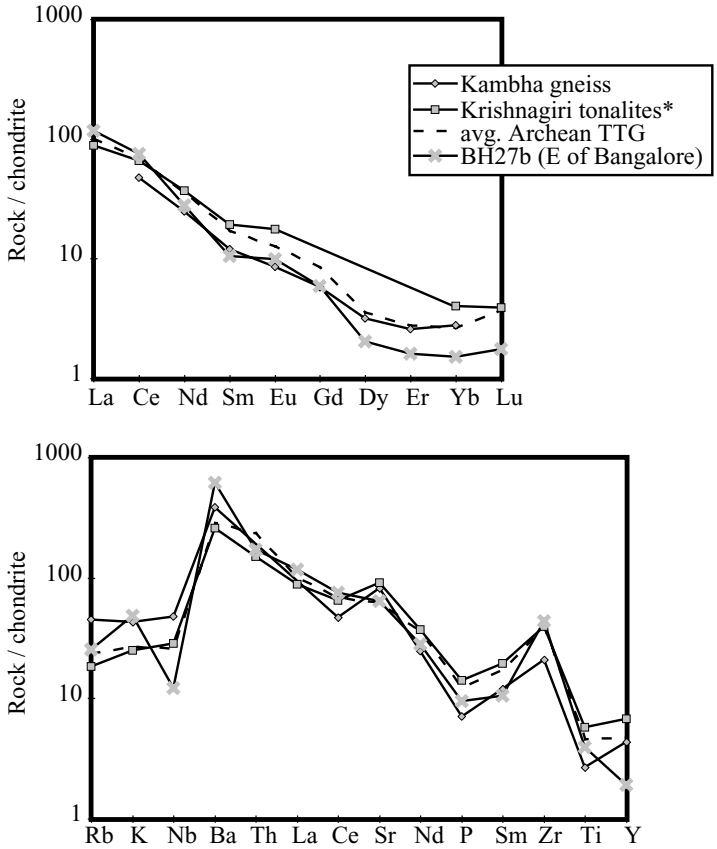

Fig. 3. REE patterns and trace element characteristics for Late Archaean TTG in the Dharwar Craton. Normalization to chondrites (Sun and McDonough, 1989). Continuous lines with points: samples from the Dharwar Craton. Dotted line: average TTG of Martin, 1994 for comparison. An asterisk (*) indicates analysis from Allen, 1985.

presents specific features that have not yet been reported for Archaean granites. To avoid systematic methodological bias, this paper will only refer to the radiometric ages measured by Peucat et al. (1993) and Jayananda et al. (1995, 2000), thus allowing a comparison of ages obtained by the same method (zircon single grain evaporation), in the same laboratory.

3.1. TTG

TTG were emplaced at 3.0–2.7 Ga ("Peninsular Gneisses") and at 2.55–2.53 Ga (Peucat et al., 1993), the latter being the subject of this study. Late Archaean TTGs are mainly found in the amphibolite-granulite transition zone of Krishnagiri-Salem area, but some also occur as rounded plutons around the Kolar Schist Belt (e.g. the Kambha gneisses; Balakrishnan and Rajamani, 1987; Krogstad et al., 1991, 1995).

The Krishnagiri tonalitic gneisses are foliated, dark, fine to medium-grained (1–2 mm) gneisses, invaded by numerous plugs and sheets of the "biotite-granite" type (Fig. 2a). The tonalitic gneiss is made of 50% plagioclase ($An_{20–30}$), 25–30% quartz, 10–15% amphibole + biotite, and small amounts (5%) of K-feldspar. Magnetite, ilmenite, sphene and zircon are accessory phases (Fig. 2b; Allen, 1985).

At upper structural levels, a coarse-grained orthogneiss pluton (the Kambha gneisses of Balakrishnan and Rajamani, 1987) consists of porphyritic trondhjemite with 1–2 cm phenocrysts of plagioclase in a quartz + minor K-feldspar ± biotite and hornblende matrix. Epidote, apatite, oxides, sphene and zircon are accessory phases.

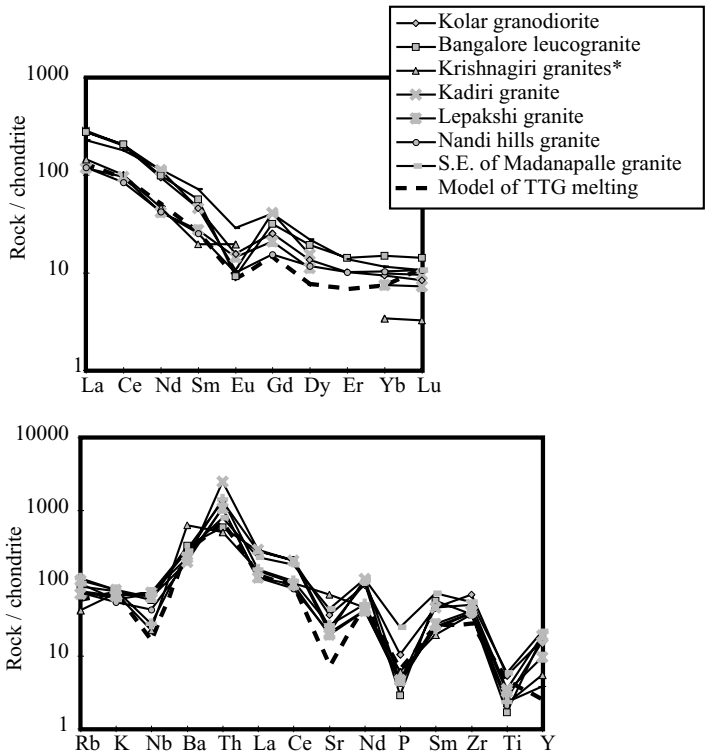

Fig. 4. Same as Fig. 3 for biotite-granites. Dotted line: model of TTG melting of Moyen et al., 2001.

Both the Krishnagiri tonalitic gneisses and the shallower plutons are typical TTG as described by Martin (1994). They have low K/Na ratios (<0.48 and more commonly <0.3), moderate Mg# (35–50), and A/CNK ≈ 1. They are moderately enriched in incompatible elements, with fractionated REE patterns ($[Ce/Yb]_N$ = 20–50), high LREE (Ce_N = 50–150), low HREE contents (Yb_N = 1–5) and slightly negative, or no, Eu anomalies (Fig. 3).

3.2. Biotite dominant granites and granodiorites

Biotite-bearing granites are typical "I-type" granites. They occur both as dykes and veins within the tonalitic gneisses of the Krishnagiri area, or as large, probably syn-tectonic plutons emplaced under amphibolite facies conditions (Subba Rao et al., 1992a,b). Some plutons between Bangalore and the Kolar Schist belt have been dated at 2540 ± 4 Ma and 2539 ± 11 Ma (Jayananda et al., 2000).

The biotite-dominant granites are generally medium to coarse-grained, white to light grey monzogranites and granodiorites. Several intrusions are porphyritic, with 1–3 cm K-feldspar phenocrysts in a 1–2 mm matrix. Major phases are K-feldspar, quartz, plagioclase ($An_{10–15}$), and biotite (less than 5%), with subordinate hornblende. Accessory phases are sphene, apatite, zircon, magnetite and ilmenite (Fig. 2c and d).

Biotite-dominant granites are slightly peraluminous (1 < A/CNK < 1.1), with high K/Na ratios (never <0.6 and commonly >1) and low Mg# (<35). They are Ni- and Cr-poor (<16 and <35 ppm, respectively), but rich in Rb (100–300 ppm) and Th (10–40 ppm). Their incompatible element patterns (Fig. 4) display positive Th and negative Sr, P and Nb anomalies. They are REE-rich (Ce_N = 50–200, Yb_N = 5–10) with moderately fractionated patterns ($[Ce/Yb]_N$ = 10–35) and significant negative Eu anomalies (Fig. 4).

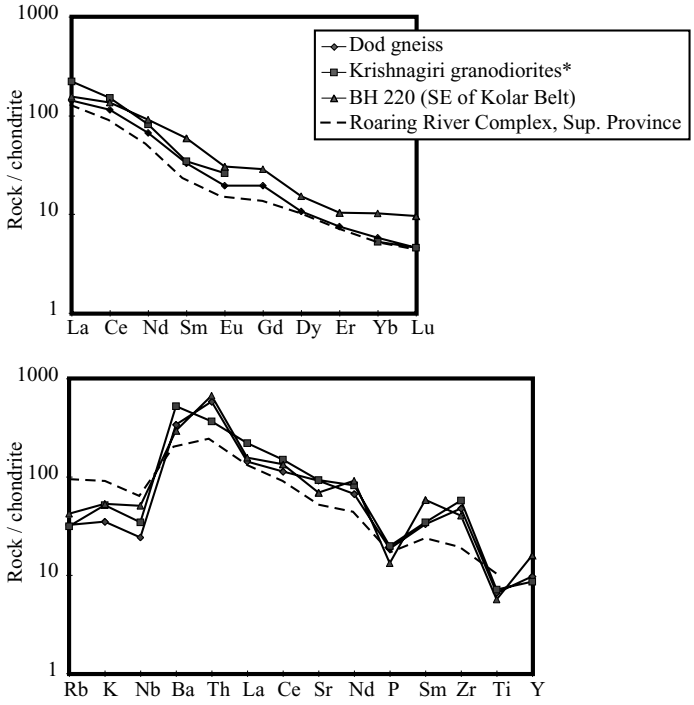

Fig. 5. Same as Fig. 3 for sanukitoids. Dotted line: Roaring River complex (Stern, 1989).

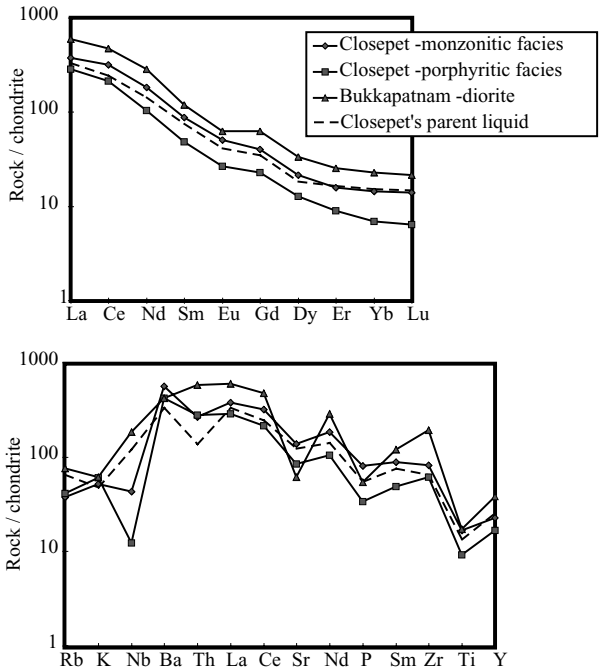

Fig. 6. Same as Fig. 3 for Closepet-type granites. Dotted line: Closepet parental liquid as calculated by Moyen et al., 2001.

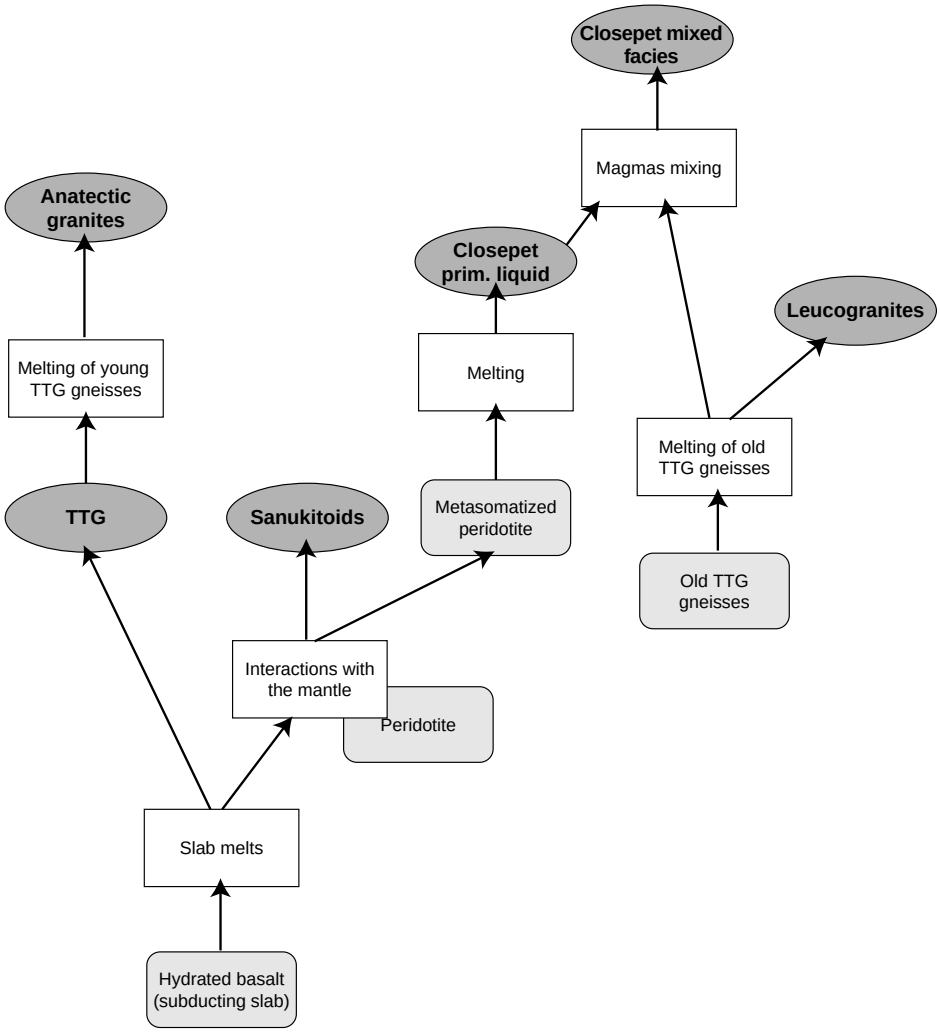

Fig. 7. Sketch summarizing the proposed petrogenetic model for the four granite types observed in the Dharwar Craton.

3.3. *Sanukitoids*

Sanukitoids occur as small plutons around the Kolar schist belt and include the 2552 ± 2 Ma "Dod gneisses" and the "Bisanattam granite" (Balakrishnan and Rajamani, 1987; Krogstad et al., 1991, 1995; Jayananda et al., 2000).

The sanukitoids are medium-grained, equant monzodiorites to granodiorites, containing distinctive 5–10 mm clusters of biotite, hornblende and rare relict hornblende-rimmed clinopyroxene. Microgranular, mafic dioritic to monzodioritic enclaves are common. The paragenesis consists of quartz, plagioclase ($An_{20–30}$), perthitic microcline, hornblende and biotite. Accessory phases are magnetite, ilmenite, epidote, sphene, apatite, zircon and allanite (Fig. 2e and f).

Sanukitoids are moderately potassic ($0.4 < K/Na < 0.6$) and have A/CNK ratios ≈1. Mg# is rather high (45–75), as are Ni and Cr contents (20–40 and 20–100 ppm, respectively). Incompatible element and REE patterns are broadly similar to those of the TTG rocks, albeit with slightly higher contents (e.g. $Ce_N = 100–200$) (Fig. 5).

3.4. The Closepet Granite

The large, 2518 ± 5 Ma (Jayananda et al., 1995) Closepet Granite represents a distinct Archean granite-type and is made up of several cogenetic phases. The dominant phase (75%) is porphyritic monzogranite, with large (commonly 2–5 cm, but occasionally up to 10 cm) phenocrysts of K-feldspar in a coarse-grained matrix of quartz, perthitic microcline, plagioclase ($An_{20–30}$), biotite and amphibole. Accessory minerals magnetite, ilmenite, zircon, large, rarely subhedral sphene, allanite and apatite are always very abundant (Fig. 2g and h).

This phase is associated with migmatites and anatectic granites derived from the surrounding Peninsular Gneisses (Jayananda et al., 1995; Moyen, 2000; Moyen et al., 2001), which are similar to the biotite-granites found elsewhere in the craton.

Large, dioritic to monzonitic, comagmatic (Jayananda et al., 1995) enclaves are found within the porphyritic monzogranite (Fig. 2g). These enclaves are fine-grained (0.1–1 mm), with rare K-feldspar phenocrysts that show reaction rims with their monzonitic host. Major mineral phases are plagioclase ($An_{20–35}$, 30–45%), perthitic microcline (15–20%), amphibole (5–30%; edenitic hornblende: Jeanningros, 1998), biotite (5–10%) and quartz. In some places, relict clinopyroxene (diopside) occurs within amphibole grains, leading Jayananda et al. (1995) to propose the name "clinopyroxene-bearing monzonite" for this phase. Accessory minerals are the same as in the host monzogranite and are still abundant, despite the relatively low SiO_2 contents of the monzonites.

Jayananda et al. (1995) and Moyen et al. (2001) demonstrated that the Closepet Granite formed by mixing of various proportions of an anatectic melt (partial melting of Peninsular Gneisses) with a mantle-derived melt (monzonitic to dioritic). The following discussion will therefore focus on the most primitive, mantle-derived liquid, so that only the source-related characteristics, rather than those of the crustal melts, are considered.

The most primitive clinopyroxene-bearing monzonites are silica-poor (50–55% SiO_2), but have rather high K/Na ratios (0.45–0.9), uncommon for such mafic rocks. They are metaluminous (A/CNK = 0.85–1) and have high Mg# (35–70). In spite of the low silica contents, clinopyroxene-bearing monzonites are REE-rich (Ce_N = 150–400, Yb_N = 5–20), with fractionated REE patterns ($[Ce/Yb]_N$ = 10–50) and no significant Eu anomalies (Fig. 6). They are extremely rich in LILE with Ba and Sr up to 2500 and 1500 ppm, respectively, at 50–55% SiO_2. Little or no marked negative Nb, Zr, Ti or Y anomalies are observed, and these rocks thus have similar trace element characteristics to Niobium-enriched basalt (NEB; Sajona et al., 1996). While the Closepet Granite bears some similarities with sanukitoids, it is more potassic, less aluminous, and with distinctive high-HFSE contents ("NEB-signature") at comparable SiO_2 contents.

The same geochemical characteristics are found in the dominant porphyritic monzogranite phase, to a lesser degree. However, its geochemical features are intermediate between those of the "true" Closepet-type granite and biotite-bearing granite as a result of mixing of clinopyroxene-bearing monzonite and anatectic granite.

4. Petrogenesis

4.1. TTG

It is now generally agreed that TTG magmas are generated by partial melting of hydrated basalt within the garnet stability field (>80 km; Martin, 1986, 1994; Drummond and Defant, 1990; Peacock et al., 1994; Rapp, 1994). In addition, Martin and Moyen (2002) evidenced a progressive increase in Ni and Cr contents of TTG from the early to the Late Archaean, which they interpreted as proof of interaction of most TTG magmas—especially the Late Archaean ones—with mantle peridotite, very probably during their ascent.

4.2. Biotite-bearing granites

Subba Rao et al. (1992a,b) concluded that some of the Dharwar Craton biotite-bearing granites formed by anatexis of a TTG-like source (either the old Peninsular Gneisses, or the younger "Krishnagiri-type" TTG). The geochemical characteristics of these rocks are in good agreement with such a conclusion (high A/CNK and K/Na, positive Rb and Th anomalies, negative Eu anomalies, etc.). Geochemical modelling

of the Closepet Granite indicated that the anatectic components of this granite were produced by water-saturated partial melting of Peninsular Gneisses (Moyen et al., 2001). However, most biotite-bearing granites, had slightly negative to positive ε_{Nd} values at 2.5 Ga (Jayananda et al., 2000), indicating that their source did not have a long crustal residence time. Consequently, it is likely that most biotite-dominant granites formed by remelting of the newly accreted TTG-type rocks.

4.3. Sanukitoids and Closepet-type granites

The sanukitoid and Closepet-type granites will be discussed together as they show several petrological and geochemical similarities. In both cases, two components were clearly involved: (1) a mantle source to produce the mafic magmas and explain the high Mg# Ni and Cr contents; and (2) a TTG-like component to account for the typical fractionated REE patterns.

Two contrasting petrogenetic models have been proposed for sanukitoid genesis. (1) Smithies and Champion (1999) considered that sanukitoids are produced by melting of a mantle source that has been transformed by assimilation of TTG melts. (2) Rapp et al. (2000) proposed that a TTG-like melt rising through peridotite is able to assimilate olivine, resulting in an "hybridised slab melt" whose chemical characteristics are very similar to sanukitoids.

Geochemical modelling by Moyen et al. (2001) demonstrated that the source for Closepet monzonitic magmas was an enriched amphibole + phlogopite + garnet + jadeitic clinopyroxene-bearing lherzolite. Such mineralogy is not commonly found in mantle lherzolites, but closely resembles the composition of the peridotite that was transformed by interactions with TTG melts in the Rapp et al. (2000) experiments. For this reason, we prefer the second petrogenetic model for the sanukitoids. The petrogenesis of both granite types can then be described as follows: hydrated basalt melted under garnet stability conditions, leading to the formation of TTG-like magmas. Reactions of such a TTG melt with the overlying peridotite during ascent produced both a hybridised sanukitoid melt and a metasomatized, jadeite-bearing lherzolite, subsequent melting of which generated the monzonitic parent magma of the Closepet-type granites. This process is rather similar to that proposed by Sajona et al. (1996) for modern "NEB" associated with adakites in the Philippines. Dating of individual intrusions (Jayananda et al., 2000) has shown that the sanukitoid intrusion of the "Dod gneisses" (2.54 Ga) slightly predates the Closepet Granite (2.52 Ga), but is synchronous with the 2.55–2.53 Ga Krishnagiri tonalitic gneisses, which is in good agreement with such a model.

5. Geodynamic implications

The biotite-bearing granites, resulting from TTG anatexis, can be produced in different geodynamic settings. However, the other three types of granitoids (TTG, sanukitoid and Closepet-type) imply more specific settings.

Recent work by Smithies (2000) and Martin and Moyen (2002) showed that most 3.0–2.5 Ga TTG had a deep-seated source, and that their parental magma interacted with mantle peridotite prior to emplacement. This geometry of peridotite above hydrated basalt is not present in the case of basaltic underplates, but corresponds to a subduction environment. Consequently, the Dharwar TTG were most likely generated in a subduction setting. Furthermore, Prouteau et al. (1999) showed that while partial melting of hydrous basalt yields TTG melts, dehydration melting of unaltered basalt leads to more granitic liquids. In a subduction setting, the basalts of the subducting slab are hydrated, which is not the case for basalts underplated below a thick crust. Finally, the modern equivalents of TTG (adakites; see Martin, 1999 for review) are only known in subduction zones. All this evidence clearly shows that TTG magmas can be considered as "slab melts", generated by partial melting of subducted oceanic crust.

Similarly, sanukitoids and Closepet-type granite genesis involves both TTG melts and mantle peridotite. However, their high MgO, Ni and Cr contents reflect more efficient interaction between TTG melt and mantle peridotite. Consequently, as their genesis necessitates a mantle wedge above the source of TTG magmas, it appears logical to conclude that they were also generated in a subduction environment. Sanukitoids are TTG melts contaminated by interaction with the mantle wedge, whereas Closepet-type magmas

were generated by fusion of a mantle metasomatized by TTG melts. In the latter case, although the mantle-enrichment is due to subduction, subsequent mantle melting is not necessarily subduction-related and could occur long after the subduction had ceased.

This model involves subduction, which implies horizontal tectonics at a plate boundary. However, this seems to contradict the detailed studies of Chardon et al. (1996, 1998), who present evidence in favour of gravity-driven tectonics ("sagduction"; cf. Gorman et al. 1978). Sagduction occurs when a dense layer (komatiites and/or banded iron formations in the greenstone belts) overlies a lighter, gneissic basement. This density inversion, associated with a higher geothermal gradient that lowers the lithosphere viscosity (Choukroune et al., 1997), resulted in sinking of the dense cover into the basement, leading to the development of a typical dome and basin pattern. This corresponds to a setting in which body forces (gravity) are dominant over boundary forces (intra-plate shortening) (Rey, 2001).

However, since our petrological and geochemical study requires the involvement of a subduction zone, it is necessary to reconcile the apparently contradictory conclusions. We propose that the two episodes were not synchronous, but occurred in close temporal succession: subduction at a plate boundary, leading to the formation of TTG and sanukitoids occurred until 2.54 Ga, followed by the closure of the oceanic domain, arc-continent collision, and assembly of a protocontinent. Subsequent reworking and deformation in an intra-continental environment at 2.52 Ga was dominated by gravitational inversion. During this second event, partial melting of the enriched mantle produced the Closepet parent magmas. Thus, the period 2.54–2.52 Ga in the Dharwar Craton likely records a transition from a plate boundary to an intra-plate setting, as well as a magmatic source transition from pure slab melts towards strongly contaminated mantle (Choukroune et al., 1997).

This two-stage process resulted in a craton where the dominant structures are clearly related to gravity-driven tectonics, but where the lithologies were controlled by plate boundary (subduction zone) processes. The proposed evolution can logically account for the apparent contradiction, and the model

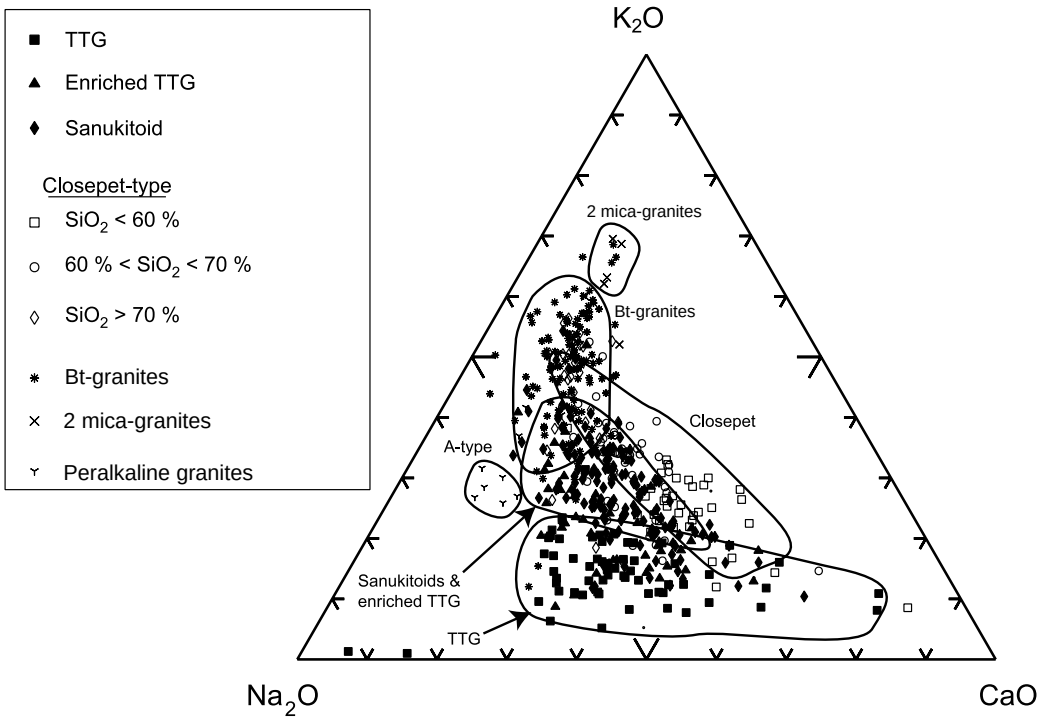

Fig. 8. Triangular K_2O–Na_2O–CaO diagram for over 500 analysis of Late Archaean granitoids worldwide (references and comments in text).

could well be applicable to other cratons where similar problems of interpretation have arisen.

6. Towards a worldwide typology

A granite typology, based on the well-exposed Dharwar Craton, can be tentatively applied to the Late Archaean of rest of the world. Approximately 500 analyses of global Late Archaean granitoids have been compiled (see references in Section 1), and the results (discussed below) show that the proposed classification into six types has a more global and general significance. Discriminant diagrams for major (Figs. 8 and 9) and trace (Fig. 10) elements show that, although there is some overlap between the groups, it is nevertheless possible to identify each type. Consequently, it must be stressed that mineralogy (Table 1), combined with major element chemistry (Figs. 8 and 9) are frequently sufficient to discriminate these granites and to provide genetic hypotheses.

While anatectic biotite-granites, TTG and sanukitoids are generally described as such in the literature, "Closepet-type" granites have hitherto not been recognised as a distinct type. They have either been described as sanukitoids (Icarus monzodiorite, Wawa subprovince, Superior Province: Shirey and Hanson, 1984, 1986; Eye Dashwa granodiorite, Wabigoon subprovince, Superior Province: Shirey and Hanson, 1984; Stevenson et al., 1999), or simply described as porphyritic, LILE-enriched diorites or granodiorites (Bridger batholith, Wyoming: Frost et al., 1998; Puzhaosi diorites, Taishan complex, China: Jahn et al., 1988). We identified and selected them from the literature on the basis of petrographic features (diorites to granodiorites, highly porphyritic, with

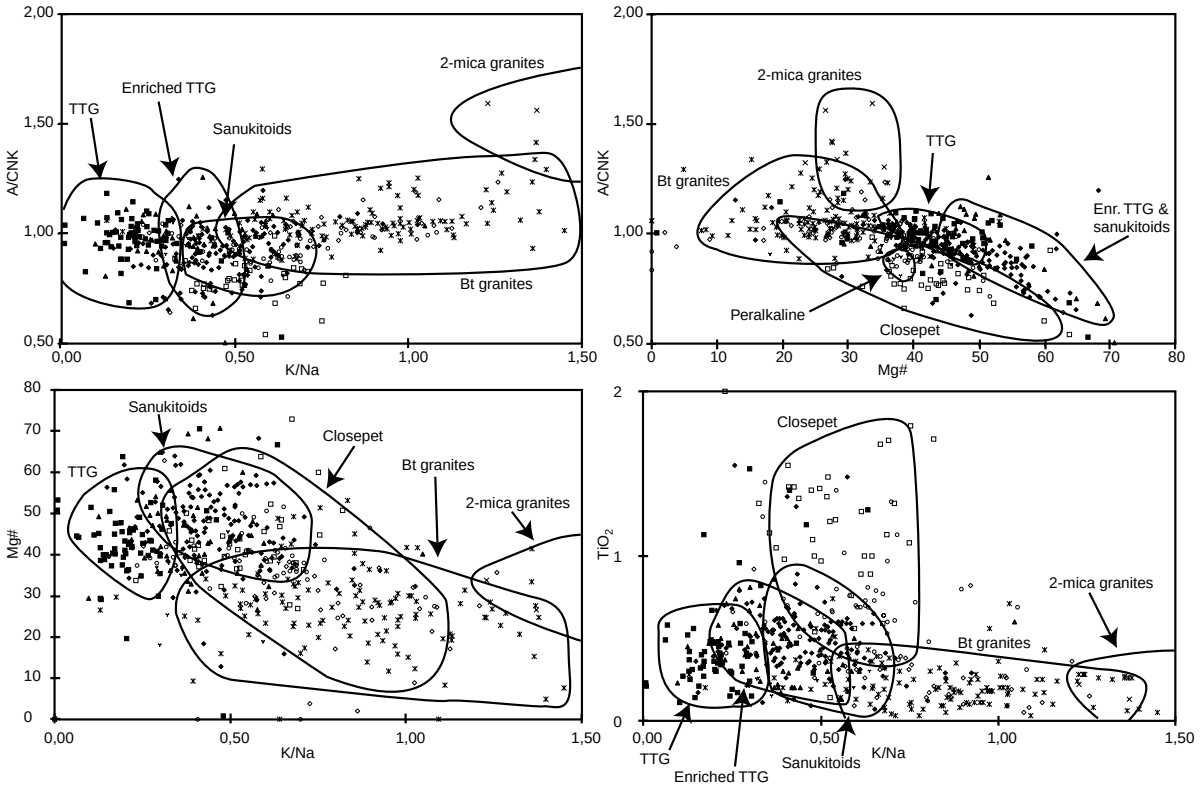

Fig. 9. Binary diagrams with major element and major element ratio for over 500 analysis of Late Archaean granitoids worldwide (references and comments in text). Mg# molecular ratio Mg/(Mg + Fe); A/CNK molecular ratio Al/(Ca + Na + K); K/Na molecular ratio. Same symbols as Fig. 8. Enr. TTG: enriched TTG.

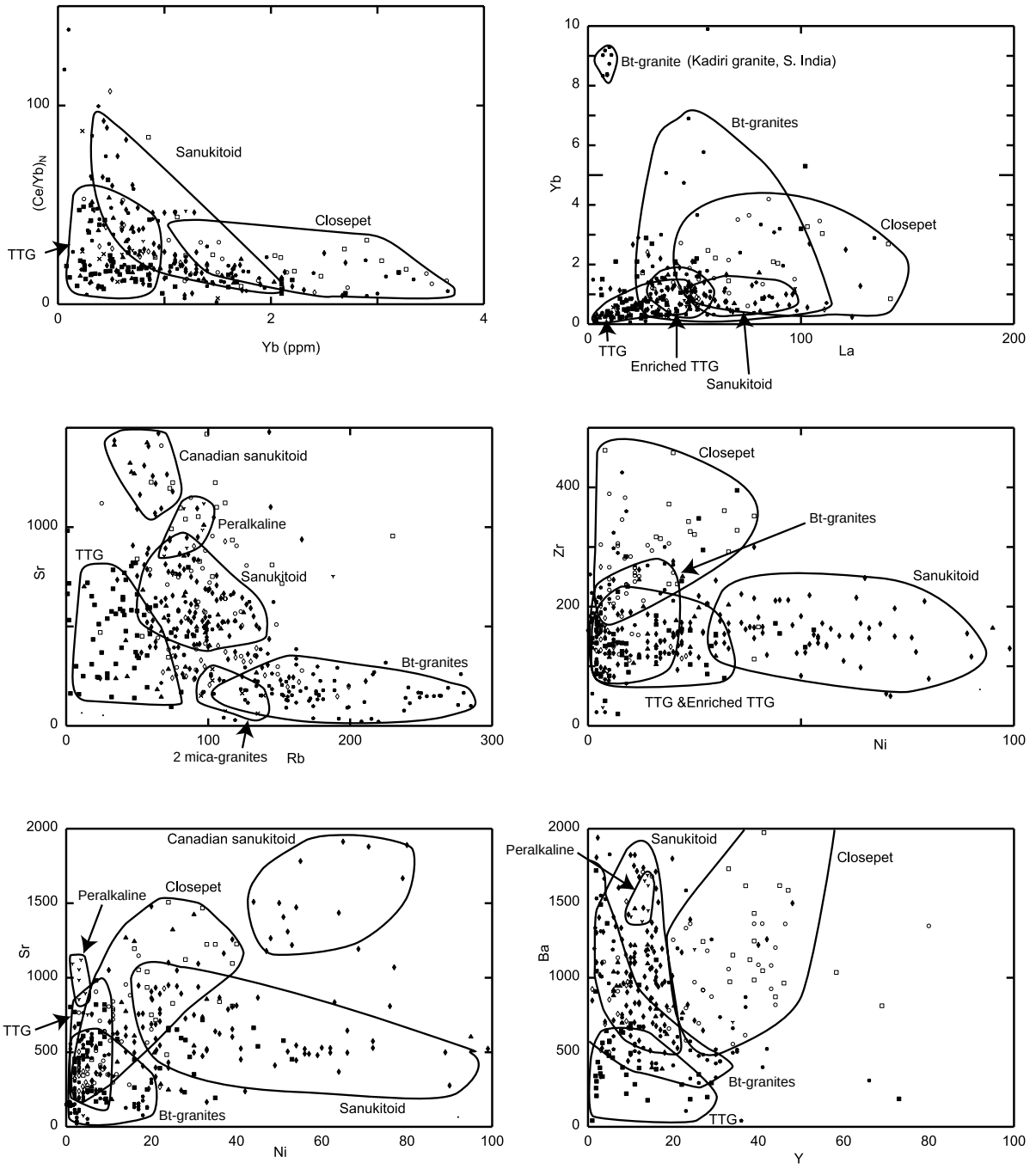

Fig. 10. Same as Fig. 9 for trace elements.

abundant accessory minerals including sphene) and geochemistry (LILE enriched, high Ni, Cr, HFSE and REE contents, high Mg#).

We have also identified two additional types of granite that were not reported in the Dharwar Craton: two-micas leucogranites, and A-type, generally peralkaline granites. Their characteristics are summarized in Tables 1 and 2.

It appears that a progressive compositional change exists from typical TTG to sanukitoids, via a group of "enriched TTG". This observation is important, as it emphasizes a genetic link between TTG and sanukitoids, with a compositional continuum between the two end-members, which are "pure" slab melts (TTG) and strongly hybridised slab melts (sanukitoids).

A-type granites are identified by their low K/Na combined with high total alkali contents, together with a distinctive mineralogy marked by the presence of alkali pyroxene and amphibole. High K/Na and low Mg# characterize the "anatectic" family. Within the "subduction" group (TTG, sanukitoids and Closepet-type), a progressive evolution is observed from TTG to sanukitoids to Closepet-type, marked by a progressive decrease of A/CNK and increase of K/Na ratios (Fig. 10).

The anatectic group is clearly identified in trace element diagrams by its high Rb and Th and low Ni and Cr contents. A distinctive feature of the Closepet-type within the "subduction" group is its consistent enrichment in all HFSE (Ti, Y, Zr and Nb). Sanukitoids have high Ni and Cr contents, while high LILE (Ba and Sr) contents are characteristic of both sanukitoids and Closepet-type.

In most Archaean cratons, TTGs are the earliest felsic components, whereas sanukitoids and Closepet-like granites represent late plutonism. TTG are 4.0–2.5 Ga, while sanukitoids and Closepet-like magmatism are mostly restricted to the Late Archaean (2.7–2.5 Ga). Rapp et al. (2000) proposed that the behaviour of slab melts mainly depends on the slab melt to mantle peridotite ratio. When this ratio is low, all slab melt is consumed in reactions with the mantle, but when this ratio is high, slab melt is only partly involved in mantle metasomatism and the other part can be emplaced as more or less mantle-contaminated magma. Martin and Moyen (2002) demonstrated that, over the Archaean, the depth of slab melting increased and, as the overlying mantle wedge thickness increased, mantle contamination of the slab melts also increased.

Thus, we propose that when Earth heat production was high in the Early to Middle Archaean, the geothermal gradients in subduction zones were high, leading to high degrees of melting of the subducted slab. Melting occurred at shallow depths and mantle contamination was not very efficient, so that emplacement of TTG magmas was favoured. Over time, heat production decreased, so that geothermal gradients decreased, and only small degrees of slab melting were possible. Most of the slab melts were consumed by reactions with the mantle wedge. Moreover, because of the greater depth of slab melting, any slab melt not consumed in mantle metasomatism had to rise through a thicker mantle wedge, thus becoming highly contaminated. Such melts could generate sanukitoids or the Late Archaean contaminated TTG (Martin and Moyen, 2002), whereas melting of the metasomatized mantle could generate Closepet-type magmas.

7. Conclusions

Late Archaean granitoids can be classified in six categories: TTG, sanukitoid, two-mica, biotite-bearing, "A-type" and high-Mg, high-HFSE ("Closepet-type"). Four of these types are found in the Dharwar Craton.

The petrogenesis of some of these granite types is relatively well constrained. Biotite-granites and two-mica granites are crustal melts (remelting of TTG and metasediments, respectively). TTGs are partial melts of hydrous basalt, in the garnet stability field. Both sanukitoids and Closepet-type granites require a mantle component, as well as a TTG component in their deep source. The favoured model for the genesis of these granite types is a three-stage evolution: (i) melting of a subducted basaltic slab in the garnet stability field; (ii) interaction of the resulting melt with mantle peridotite during its ascent, yielding sanukitoid magmas, together with a hybridised mantle; (iii) remelting of the hybridised mantle forming parental liquids of the Closepet-type.

The petrogenetic model for EDC granites implies both subduction and post-subduction geodynamic settings. TTGs and sanukitoids are generated during the first subduction-related stage, whereas the sub-

sequent stage is associated with terrane accretion or small-scale collision and produces biotite-granites and "Closepet-type" granites. This model could account for the apparent contradiction found in most Archaean cratons between clearly subduction-related lithologies, and structures that can only be interpreted as gravity-driven.

Archaean anatectic and peralkaline granites have modern counterparts, but not TTG, sanukitoids and Closepet-type granites (except in rather unusual settings, adakites for instance). Typical Phanerozoic calc-alkaline granites related to subduction zones are essentially lacking in the Archaean. This suggests that crustal accretion processes, operating at convergent margins, were different in the Archaean.

The secular evolution of global Archaean magmatism could reflect the progressive cooling of our planet. After 2.5 Ga, Earth cooling induced low geothermal gradients in subduction zones, so that slab melting became subordinate to slab dehydration, leading to the classical calc-alkaline magmatism of Proterozoic to Phanerozoic times.

Acknowledgements

Fieldwork and analyses were funded by IFCPAR (project 2307-1). JFM's participation to the 4th IAS meeting was partially funded by a J.H Lord travel grant, and a CNFG grant. Authors are thankful to M.J. Van Kranendonk, who invited us to contribute to the "special issue" and helped clarify the manuscript. Fruitful discussions with R.H. Smithies and D. Champion during the 4th IAS meeting are also acknowledged. Reviews by J. Sheraton and D. Champion were greatly thought provoking and stimulating, and greatly helped in improving the syntax and English of the manuscript.

References

Albarède, F., 1998. The growth of continental crust. Tectonophysics 196, 1–14.

Allen, P., 1985. The Geochemistry of the Amphibolite-Granulite Facies Transition in Central South India. Unpublished Ph.D. thesis, New Mexico Institute of Mining & Technology, Socorro, NM.

Allen, P., Condie, K.C., Narayana, B.L., 1985. Geochemistry of the prograde and retrograde charnockite-gneiss reactions in South India. Geochim. Cosmochim. Acta 49, 323–339.

Atherton, M.P., Petford, N., 1993. Generation of sodium-rich magmas from newly underplated basaltic crust. Nature 362, 144–146.

Balakrishnan, S., Rajamani, V., 1987. Geochemistry and petrogenesis of granitoids around the Kolar Schist belt, South India: constraints for the evolution of the crust in the Kolar area. J. Geol. 95, 219–240.

Berger, M., Rollinson, H.R., 1997. Isotopic and geochemical evidence for crust–mantle interaction during Late Archaean crustal growth. Geochim. Cosmochim. Acta 61, 4809–4829.

Bourne, J.H., L'Heureux, M., 1991. The petrography and geochemistry of the Clericy pluton: an ultrapotassic pyroxenite-syenite suite of Late Archaean age from the Abitibi region, Quebec. Precambrian Res. 52, 37–51.

Chadwick, B., Vasudev, V.N., Hegde, G.V., 2000. The Dharwar Craton, southern India, interpreted as the result of Late Archaean oblique convergence. Precambrian Res. 99, 91–111.

Champion, D.C., Sheraton, J.W., 1997. Geochemistry and Nd isotope systematics of Archaean of the Eastern Goldfields, Yilgarn Craton, Australia: implications for crustal growth processes. Precambrian Res. 83, 109–132.

Champion, D.C., Smithies, R.H., 1999. Archaean granites of the Yilgarn and Pilbara cratons, Western Australia: secular changes. In: Barbarin, B. (Ed.), The Origin of Granites and Related Rocks—IVth Hutton Symposium Abstracts Doc. BRGM 290, pp. 137.

Chardon, D., Choukroune, P., Jayananda, M., 1996. Strain patterns, decollement and incipient sagducted greenstone terrains in the Archaean Dharwar craton (South India). J. Struct. Geol. 18, 991–1004.

Chardon, D., Choukroune, P., Jayananda, M., 1998. Sinking of the Dharwar Basin (South India); implications for Archaean tectonics. Precambrian Res. 91, 15–39.

Choukroune, P., Ludden, J.N., Chardon, D., Calvert, A.J., Bouhallier, H., 1997. Archaean crustal growth and tectonic processes: a comparison of the Superior Province, Canada, and the Dharwar craton, India. In: Burg, J.-P., Ford, M. (Eds.), Orogeny Through Time, Geology Society London Special Publication, vol. 121, pp. 63–98.

Collins, W.J., 1993. Melting of Archaean sialic crust under high a_{H_2O} conditions: genesis of 3300 Ma Na-rich granitoids in the Mount Edgar Batholith, Pilbara Block, Western Australia. Precambrian Res. 60, 151–174.

Condie, K.C., 1989. Plate Tectonics and Crustal Evolution, 3rd ed. Pergamon, 476 pp.

Day, W.C., Weiblen, P.W., 1986. Origin of Late Archaean granite: geochemical evidence from the Vermilion granitic complex of Northern Minnesota. Contrib. Miner. Petrol. 93, 283–296.

Defant, M.J., Drummond, M.S., 1990. Derivation of some modern arc magmas by melting of young subducted lithosphere. Nature 347, 662–665.

De Wit, M., 2001. Archaean Tectonics: Wading Through a Mine-Field of Controversies. Australian Geological Survey Organisation, Record 2001/37, 4th International Archaean Symposium. Perth, WA, p. 8.

Drummond, M.S., Defant, M.J., 1990. A model for trodhjemite–tonalite–dacite genesis and crustal growth via slab melting: Archaen to modern comparisons. J. Geophys. Res. 95, 21503–21521.

Frost, C.D., Frost, B.R., Chamberlain, K.R., Hulsebosch, T.P., 1998. The Late Archaean history of the Wyoming province as recorded by granitic magmatism in the Wind River Range, Wyoming. Precambrian Res. 98, 145–173.

Jahn, B., Auvray, B., Shen, Q., Zhang, Z., Dong, Y., Ye, X., Zhang, Q., Cornichet, J., Mace, J., 1988. Archaean crustal evolution in China: the Taishan complex, and evidence for juvenile crustal addition from long-term depleted mantle. Precambrian Res. 38, 381–403.

Jayananda, M., Martin, H., Peucat, J.-J., Mahabaleswar, B., 1995. Late Archaean crust-mantle interactions: geochemistry of LREE-enriched mantle derived magmas. Example of the Closepet batholith, Southern India. Contrib. Miner. Petrol. 199, 314–329.

Jayananda, M., Moyen, J.-F., Martin, H., Peucat, J.-J., Auvray, B., Mahabaleswar, B., 2000. Late Archaean (2550–2520 Ma) juvenile magmatism in the Eastern Dharwar craton, southern India: constraints from geochronology, Nd–Sr isotopes and whole rock geochemistry. Precambrian Res. 99, 225–254.

Jeanningros, A., 1998. Etude pétrologique, minéralogique et géochimique des phénomènes de mélange magmatique dans le granite de Closepet (Inde). Mem. Maîtrise, Univ. B. Pascal, Clermont-Ferrand, France, 26 pp.

Krogstad, E.J., Balakrishnan, S., Mukhopadhyay, D.K., Rajamani, V., Hanson, G.V., 1989. Plate tectonics 2.5 billion years ago: evidence at Kolar, South India. Science 243, 1337–1340.

Krogstad, E.J., Hanson, G.N., Rajamani, V., 1991. U–Pb ages of zircon and sphene for two gneiss terranes adjacent to the Kolar schist belt, South India: evidence for separate crustal evolution histories. J. Geol. 99, 801–816.

Krogstad, E.J., Hanson, G.N., Rajamani, V., 1995. Sources of continental magmatism adjacent to the late Archean Kolar Suture Zone, South India: distinct isotopic and elemental signatures of two late Archean magmatic series. Contrib. Miner. Petrol. 122, 159–173.

Laflèche, M.R., Dupuy, C., Dostal, J., 1991. Archaean orogenic ultrapotassic magmatism: an example from the southern Abitibi greenstone belt. Precambrian Res. 52, 71–96.

Martin, H., 1986. Effect of steeper Archean geothermal gradient on geochemistry of subduction-zone magmas. Geology 14, 753–756.

Martin H., 1994. The Archean grey gneisses and the genesis of continental crust. In: Condie K.C. (Ed.), Archean Crustal Evolution. Developments in Precambrian Geology, vol. 11, Chapter 6, pp. 205–260.

Martin, H., 1999. The adakites: modern analogs of Archaean granitoids. Lithos. 46, 411–429.

Martin, H., Moyen, J.-F., 2002. Secular changes in TTG composition as markers of the progressive cooling of the Earth. Geology, in press.

Moyen, J.-F., 2000. Le magmatisme granitique à la transition Archéen-protérozoïque: exemple du Craton de Dharwar, Inde du Sud (granite de Closepet et intrusions associées). Ph.D. thesis, Univ. B. Pascal, Clermont-Ferrand, France, 487 pp.

Moyen, J.-F., Martin, H., Jayananda, M., 2001. Multi-elements geochemical modelling during Late Archaean crustal growth: the Closepet Granite (South India). Precambrian Res. 112, 87–105.

Moyen, J.-F., Nédélec, A., Martin, H., Jayananda, M., 2003. Syntectonic granite emplacement at different structural levels: the Closepet Granite, South India. J. Struct. Geol. 25, 611–631.

Peacock, S.M., Rushmer, T., Thompson, A.B., 1994. Partial melting of subducting oceanic crust. Earth Planet. Sci. Lett. 121, 24–227.

Peucat, J.-J., Mahabaleswar, M., Jayananda, M., 1993. Age of younger tonalitic magmatism and granulite metamorphism in the amphibolite-granulite transition zone of southern India (Krishnagiri area): comparison with older Peninsular gneisses of Gorur-Hassan area. J. Metam. Geol. 11, 879–888.

Prouteau, G., Scaillet, B., Pichavant, M., Maury, R.C., 1999. Fluid-present melting of ocean crust in subduction zone. Geology 27, 1111–1114.

Querré, G., 1985. Palingenèse de la croûte continentale à l'Archéen: les granitoïdes tardifs (2.5–2.4 Ga) de Finlande Orientale. Ph.D. thesis, Univ. Rennes-1, France.

Raase, P., Raith, M., Ackermand, D., Lal, R.K., 1986. Progressive metamorphism of mafic rocks from greenschist facies to granulite facies in the Dharwar craton of southern India. J. Geol. 94, 261–282.

Rapp, R.P., 1994. Partial melting of metabasalts at 2–7 GPa: experimental results and implications for lower crustal and subduction zone processes. Miner. Mag. 58A, 760–761.

Rapp, R., Shimizu, N., Norman, M.C., Applegate, G.S., 2000. Reaction between slab-derived melts and peridotite in the mantle wedge: experimental constraints at 3.8 GPa. Chem. Geol. 160, 335–356.

Rey, P., 2001. The Impact of Body Forces on the Archaean Continental Lithosphere. Australian Geological Survey Organisation, Record 2001/37, 4th International Archaean Symposium. Perth, WA, pp 145–146.

Rollinson, H., 1997. Eclogite xenoliths in west African kimberlites as residues from Archaean granitoid crust formation. Nature 389, 173–176.

Rollinson, H.R., Windley, B.F., Ramakrishnan, M., 1981. Contrasting high and intermediate pressures of metamorphism in the Archaean Sargur schists of southern India. Contrib. Miner. Petrol. 76, 420–429.

Rudnick, R.L., 1995. Making continental crust. Nature 378, 571–577.

Sajona, F.G., Maury, R.C., Bellon, H., Cotten, J., Defant, M.J., 1996. HFSE enrichment of Pliocene-Pleistocene island arc basalts, Zamboanga Peninsula, Western Mindanao (Philippines). J. Petrol. 37, 693–726.

Sen, C., Dunn, T., 1994. Experimental modal metasomatism of a spinel lherzolite and the production of amphibole-bearing peridotite. Contrib. Miner. Petrol. 119, 422–432.

Shirey, S.B., Hanson, G.N., 1984. Mantle-derived Archaean monzodiorites and trachyandesites. Nature 310, 222–224.

Shirey, S.B., Hanson, G.N., 1986. Mantle heterogeneity and crustal recycling in Archaean granite-greenstone belts: evidence from

Nd isotopes and trace elements in the Rainy Lake area, Superior Province, Ontario, Canada. Geochim. Cosmochim. Acta 50, 2631–2651.

Smithies, R.H., 2000. The Archaean tonalite–trondhjemite–granodiorite (TTG) series is not an analogue of Cenozoic adakite. Earth Planet. Sci. Lett. 182, 115–125.

Smithies, R.H., Champion, D.C., 1999. Archaean high-Mg diorite (sanukitoid) suite, Pilbara Craton, Western Australia: petrogenesis and links to tonalite–trondhjemite–granodiorite and alkaline magmatism. J. Petrol. 41, 1653–1671.

Stern, R.A., 1989. Petrogenesis of Archaean Sanukitoid Suite. Ph.D. thesis, State University of New York at Stony Brook, 275 pp.

Stern, R.A., Hanson, G., 1991. Archaean high-Mg granodiorites: a derivative of light rare earth enriched monzodiorite of mantle origin. J. Petrol. 32, 201–238.

Stern, R.A., Hanson, G.N., Shirey, S.B., 1989. Petrogenesis of mantle-derived, LILE- enriched Archean monzodiorites and trachyandesites (sanukitoids) in Southwestern Superior Province. Can. J. Earth Sci. 26, 1688–1712.

Stevenson, R., Henry, P., Gariépy, C., 1999. Assimilation-fractional crystallization origin of Archaean sanukitoid suites: Western Superior Province, Canada. Precambrian Res. 96, 83–99.

Subba Rao, M.V., Divakara Rao, V., Balaram, V., Ganeshwara Rao, T., 1992a. Source characteristics, petrogenesis and evolution of the LILE-enriched granitic terrain of the Kadiri region in Anantapur district, Andhra Pradesh. In: Proceedings of the 28th Annual Convention and the Seminar on Geophysics for Rural Development, December 1991, Hyderabad, India, pp. 108–117.

Subba Rao, M.V., Divakara Rao, V., Govil, P.K., Balaram, V., Pantulu, G.V.C., 1992b. Geochemical and Sr isotopic signatures in the 2.6 By Lepakshi granite, Anantapur district Andhra Pradesh: implications for its origin and evolution. Indian Miner. 46, 289–302.

Sun, S.S., McDonough, W.F., 1989. Chemical and isotopic systematics of oceanic basalts: implications for mantle composition and processes. In Magmatism in Ocean Basins. Geol. Soc. Sp. Publ. Lond. 42, 313–345.

Sylvester, P.J.,1994. Archaean granite plutons. In: Condie, K.C. (Ed.), Archaean Crustal Evolution. Developments in Precambrian Geology, vol. 11. Elsevier, Amsterdam, pp. 261–314.

Windley, B.F, 1995. The Evolving Continents, 3rd ed. Chester, John Wiley, 526 pp.

Zamora, D., 2000. Fusion de la croûte océanique subductée: approche expérimentale et géochimique. Université Thesis, Université Blaise Pascal, Clermont-Ferrand, 314 pp.